REPORT DOCUMENTATION PAGE

Form Approved OMB NO. 0704-0188

1. REPORT DATE (DD-MM-YYYY)	2. REPORT TYPE	3. DATES COVERED (From - To)
	Technical Report	-

4. TITLE AND SUBTITLE
W91NF1310107 Progress Report for 10/01/2013 ~ 9/30/2014

5a. CONTRACT NUMBER
W911NF-13-1-0107

5b. GRANT NUMBER

5c. PROGRAM ELEMENT NUMBER

6. AUTHORS

5d. PROJECT NUMBER

5e. TASK NUMBER

5f. WORK UNIT NUMBER

7. PERFORMING ORGANIZATION NAMES AND ADDRESSES
IBM Corporation (Almaden Research Cente
650 Harry Road

San Jose, CA 95120 -6099

8. PERFORMING ORGANIZATION REPORT NUMBER

9. SPONSORING/MONITORING AGENCY NAME(S) AND ADDRESS (ES)
U.S. Army Research Office
P.O. Box 12211
Research Triangle Park, NC 27709-2211

10. SPONSOR/MONITOR'S ACRONYM(S)
ARO

11. SPONSOR/MONITOR'S REPORT NUMBER(S)
63248-CS-ACI.3

12. DISTRIBUTION AVAILIBILITY STATEMENT
Approved for public release; distribution is unlimited.

13. SUPPLEMENTARY NOTES
The views, opinions and/or findings contained in this report are those of the author(s) and should not contrued as an official Department of the Army position, policy or decision, unless so designated by other documentation.

14. ABSTRACT
This is a technical report for the period: 10-1-2013 to 9-30-2014

15. SUBJECT TERMS
Racetrack Memory

16. SECURITY CLASSIFICATION OF:			17. LIMITATION OF ABSTRACT	15. NUMBER OF PAGES	19a. NAME OF RESPONSIBLE PERSON
a. REPORT	b. ABSTRACT	c. THIS PAGE			Stuart Parkin
UU	UU	UU	UU		19b. TELEPHONE NUMBER 408-927-2390

Standard Form 298 (Rev 8/98)
Prescribed by ANSI Std. Z39.18

Report Title

W91NF1310107 Progress Report for 10/01/2013 ~ 9/30/2014

ABSTRACT

This is a technical report for the period: 10-1-2013 to 9-30-2014

W91NF1310107 Progress Report for 10/01/2013 ~ 9/30/2014

1. Giant exchange coupling torque driven domain wall velocities in synthetic antiferromagnets

Previously we reported a novel mechanism to move domain walls with nanosecond long current pulses in perpendicularly magnetized thin films that are formed from multilayers composed of atomically thin cobalt and nickel layers, that are formed on heavy metal underlayers such as platinum (or iridium or palladium) and/or have heavy metal overlayers. This mechanism, which we entitled a chiral spin torque (CST), arises from spin-orbit interactions in perpendicularly magnetized, ultrathin films that display chiral domain walls (DWs). The chirality of the domain walls is set by an exchange interaction of magnetic layers that display perpendicular magnetic anisotropy (PMA) at the interface with the heavy metal layer. The chiral spin torque (CST) is distinct from conventional spin transfer torque (STT) and provides a very efficient mechanism to manipulate DWs motion in nanowires for Racetrack Memory, the focus of our program [1,2].

The use of high PMA significantly increases the density of the DWs that can be stored in a racetrack but the density is limited by the fringing fields from the DWs that gives rise to interactions between the DWs. To overcome this limitation we have constructed racetracks that have no net magnetization by forming them from synthetic antiferromagnets (SAF). We show not only can domain walls be moved with current in such racetracks with nano-second long current pulses but the domain walls move even faster than in nanowires which have magnetization. The SAF nano-wires are formed from synthetic antiferrromagnets, namely sandwiches of perpendicularly magnetized nano-wires coupled antiferromagnetically via ultrathin ruthenium layers. The domain walls in one layer are mirrored in the other layer. We have discovered that the large antiferromagnetic exchange-coupling that arises from the Ru layer, gives rise to a novel giant exchange coupling torque that drives the domain walls much more efficiently and at speeds several times higher than in nearly identical ferromagnetically coupled sandwiches. We have found record domain wall velocities of almost 1,000 m/s [3].

When the Co/Ni/Co films are deposited on Pt underlayers the DWs possess a chiral Néel structure due to a Dzyaloshinskii-Moriya exchange interaction (DMI) derived from strong spin-orbit coupling and a proximity induced magnetization in Pt [2]. A schematic diagram of the DW structure is shown in Fig. 1a and b for the SF (synthetic ferromagnetic) and SAF nanowires, respectively. The magnetization rotates from up (↑) to down (↓) counterclockwise in a plane parallel to the length of the nanowire such that the magnetization in the middle of the DW (M_L) is aligned along the nanowire. When the exchange coupling between the LM and UM layers is sufficiently strong the DW in the UM layer has the same chirality as that in the LM, irrespective of whether the coupling is ferromagnetic (F) or AF. Thus, for the SAF case, the moment in the middle of the ↓↑ DW in the UM (M_U) will be aligned in the opposite direction to that in the LM. As illustrated schematically in Fig. 1c and d, when current flows through the nanowire, the spin current that is generated by the spin Hall effect in the Pt layer induces a torque on the DW in the LM that results in the rotation of the DW's magnetization towards the accumulated spin direction transverse to the nanowire's length. It is predominantly this spin Hall torque (SHT) in conjunction with the DMI field torque, which results in the motion of the DW in the direction of the current along the nanowire. The magnitude of the SHT depends on the angle between M_L (or M_U) and the spin accumulation direction. As the current is increased M_L (or M_U) rotates towards the spin accumulation direction so that eventually a Bloch DW structure results in which M_L (or M_U) is oriented transverse to the nanowire and the SHT becomes zero. As a result, the DW velocity becomes saturated with the increasing current. We have determined that the SAF structure gives rise to a novel torque associated with the antiferromagnetic exchange-coupling field. This exchange-coupling torque (ECT) is about one order of magnitude larger than the DMI field torque and is key to accounting for the much higher DW velocities in the SAF racetracks.

The dependence of the DW velocity v on current density is compared in Fig. 2a for several nanowires formed from identical structures except that the Ru thickness is slightly changed from 2 Å

to 8 Å to allow for F or AF coupling. The corresponding perpendicular magnetization versus field hysteresis loops are shown in Fig. 2b. It is clear from Fig. 2a that the DW velocity is significantly higher for the SAF structures compared to the SF structure. Moreover, as the magnetization of the UM is increased to more closely compensate that of the LM, the DW velocity monotonically increases, reaching a value of value of ~750 m/sec when $M_U/M_L \sim 0.85$.

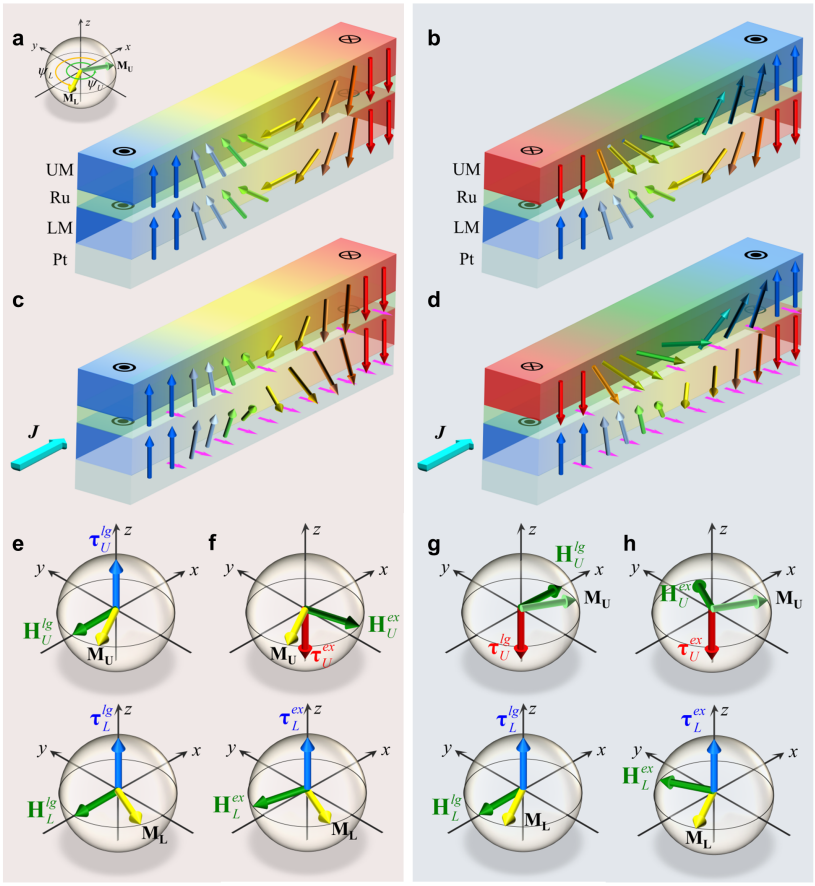

Figure 1 Schematic illustrations of the DWs in the upper (UM) and lower (LM) magnetic layers in perpendicularly magnetized SF (**a**,**c**) and SAF (**b**,**d**) nanowires for J=0 (**a**,**b**) and finite J (**c**,**d**). M_L and M_U, the magnetizations in the center of the DWs in UM and LM, respectively, exhibit an anticlockwise Néel structure when J=0. When $J \neq 0$ M_L and M_U are rotated towards the spin accumulation direction denoted by the magenta arrows and are subjected to longitudinal fields, H_L^{lg} and H_U^{lg}, respectively, that are composed of the corresponding DMI fields and H_x, and exchange-coupling fields, H_L^{ex} and H_U^{ex}, respectively. Each of these fields gives rise to a corresponding torque, namely, $\boldsymbol{\tau}_L^{\mathrm{lg}}$ and $\boldsymbol{\tau}_U^{\mathrm{lg}}$, and, $\boldsymbol{\tau}_L^{ex}$ and $\boldsymbol{\tau}_U^{ex}$. The directions of these fields and torques are shown schematically in (**e**,**f**) for the SF case and (**g**,**h**) for the SAF case. In each of these figures the upper and lower diagrams correspond to UM and LM, respectively.

The relationship of the DW velocity to M_R/M_S (M_R : remnant magnetization, M_S: saturation magnetization) is shown in Fig. 2c and d for a series of nearly identical samples in which only the Ru layer thickness t_{Ru} is varied. As the coupling through the Ru oscillates from F to AF to F the DW velocity also oscillates clearly showing that the SAF structures sustain significantly higher DW velocities compared to SF structures. A clear correlation between v and the degree to which the SAF structure is compensated is thus revealed. As the M_R/M_S is decreased from 1 (F coupling) v increases and attains a velocity of almost 800 m/sec when M_R/M_S= 0.08, which is more than 4 times higher than the velocity for the F coupled racetracks and more than 2 times higher than the highest current induced DW velocity yet reported in any racetrack.

Considerable insight into why domain walls can move much faster under chiral spin torque in

SAF compared to SF structures is obtained by developing a 1D model of the magnetization dynamics. The spin Hall torque generated in the Pt underlayer results in both M_L and M_U rotating towards the transverse direction, -y, (along the spin accumulation) although the spin current intensity in the UM will be attenuated through the thickness of the LM and the Ru layer (with attenuation lengths estimated to be ~1 nm and 4 nm, respectively). This is shown schematically in Fig. 1c and d, for the SF and SAF cases, respectively. Once M_L and M_U are rotated from their equilibrium conditions they will be subjected to several torques that include a longitudinal field torque $\boldsymbol{\tau}_i^{\mathrm{lg}}$, derived from the DMI

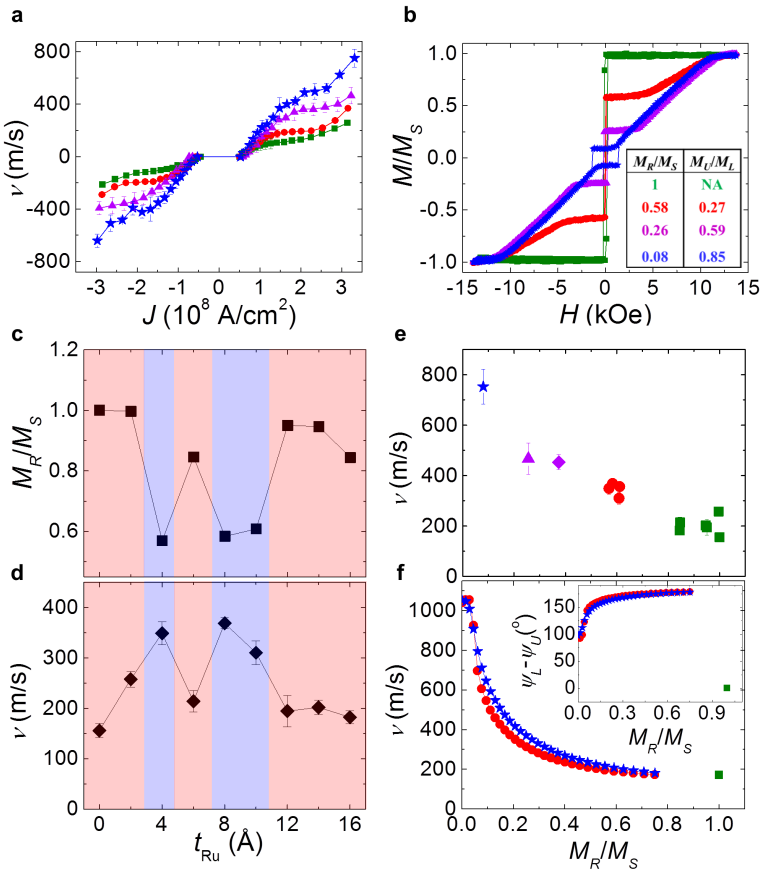

Figure 2. **a,** DW velocity v as a function of current pulse density J, and **b**, normalized perpendicular magnetization versus field hysteresis loops measured by polar Kerr magnetometer in nanowires formed from 20 TaN | 15 Pt | 3 Co | 7 Ni | 1.5 Co | t_{Ru} Ru | t_a Co | 7 Ni | t_b Co | 50 TaN where t_{Ru}=2, t_a=1.5, t_b=1.5 (green squares), t_{Ru} =8, t_a=1.5, t_b=1.5 (red circles), t_{Ru} =8, t_a=3, t_b=1.5 (violet triangles), and t_{Ru}=8, t_a=3, t_b=3 (blue stars). **c**, M_R/M_S ratio and **d**, DW velocity as a function of t_{Ru} for 20 TaN | 15 Pt | 3 Co | 7 Ni | 1.5 Co | t_{Ru} Ru | 1.5 Co | 7 Ni | 1.5 Co | 50 TaN. Red and blue shaded regions correspond to SF ($J^{ex} > 0$) and SAF ($J^{ex} < 0$), respectively. **e,** The dependence of measured DW velocity on M_R/M_S for nanowires formed from: 3 Co | 7 Ni | 1.5 Co | 0, 2, 6, 12 and 16 Ru | 1.5 Co | 7 Ni | 1.5 Co (green squares, SF); 3 Co | 7 Ni | 1.5 Co | 4,8, and 10 Ru | 1.5 Co | 7 Ni | 1.5 Co (red circles, SAF); 3 Co | 7 Ni | 1.5 Co | 8 Ru | 1.5 Co | 7 Ni | 3 Co (violet diamond, SAF); 3 Co | 7 Ni | 1.5 Co | 8 Ru | 3 Co | 7 Ni | 1.5 Co (violet triangle, SAF); 3 Co | 7 Ni | 1.5 Co | 8 Ru | 3 Co | 7 Ni | 3 Co (blue star, SAF); each with 20 TaN | 15 Pt underlayer and 50 TaN capping layer. **f**, Calculated DW velocity and $\psi_L - \psi_U$ (inset) versus M_R/M_S within the 1D model for SF nanowires. All thicknesses are in Å.

(and any longitudinal field, H_x, that might be applied, as discussed later), a damping torque that is proportional to the time derivative of M_L or M_U, and an anisotropy field derived torque. For the SAF and SF cases there is an additional torque ($\boldsymbol{\tau}_L^{ex}$ and $\boldsymbol{\tau}_U^{ex}$) derived from the exchange coupling fields (H_L^{ex} and H_U^{ex}). All of these torques are directed along the z-axis and therefore contribute to the motion of the domain wall but the damping and anisotropy field torque are small. The largest torques are the ECT (Fig. 1f,h) and the DMI torque (Fig. 1e,g) but the former is much larger in the samples studied here because the exchange coupling field is much larger than the DMI field.

However, since the sign of the ECT is opposite for the upper and lower layers for both the SF and SAF cases, the torques drive the DWs in the upper and lower layers in opposite directions in the SF case so that there is no net driving force for the composite DW (see Fig. 1d). By contrast in the SAF case these torques correspondingly drive the DWs in the upper and lower layers in the same direction and thereby provide a powerful novel driving mechanism for the composite DW (see Fig. 1h). This mechanism derives from the SAF structure. In particular this model readily accounts for the dependence of the DW velocity on the degree of compensation of the SAF structure, as shown in Fig. 2d. These data are calculated using experimentally derived properties of the Co/Ni nanowires and are in excellent agreement with our experimental data (Fig. 2c). We note that the ECT is maximized when $\psi_L - \psi_U = 90^\circ$ during the current induced motion of the DWs. The model shows that for a perfectly compensated SAF the DW velocity exceeds 1,000 m/s.

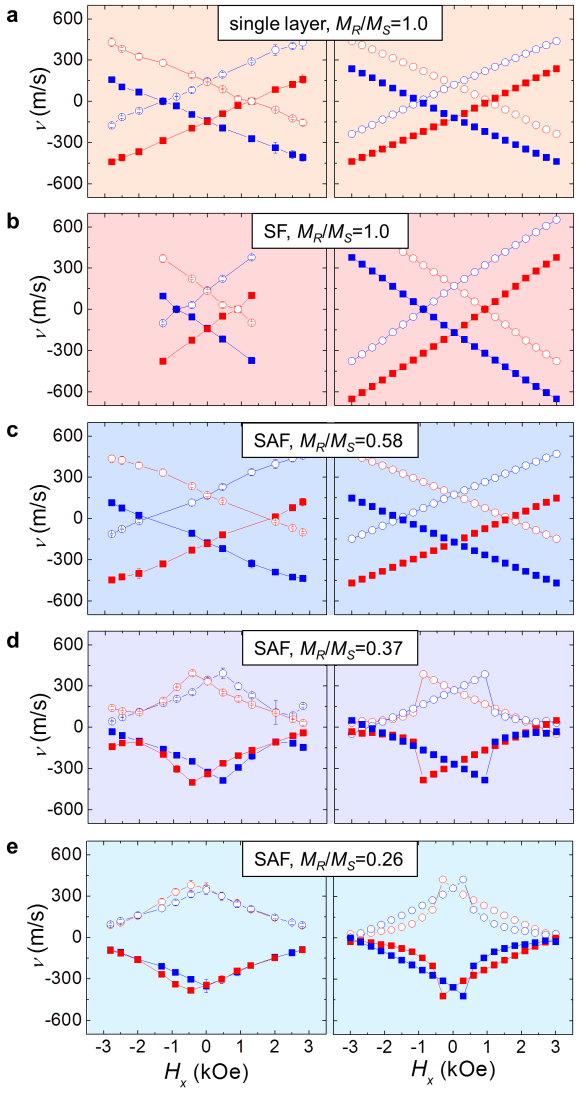

Figure 3. Left and right panels show the measured and calculated DW velocity (1D model) versus the strength of the applied longitudinal field H_x for nanowires formed from: **a,** single magnetic layer, **b,** SF structure, and **c-e**, SAF nanowires with different values of M_R/M_S. The structures are as follows: **a**, 3 Co | 7 Ni | 1.5 Co | 50 Ru; **b,** 3 Co | 7 Ni | 1.5 Co | 2 Ru | 1.5 Co | 7 Ni | 1.5 Co | 50 TaN; **c,** 3 Co | 7 Ni | 1.5 Co | 8 Ru | 1.5 Co | 7 Ni | 1.5 Co | 50 TaN; **d,** 3 Co | 7 Ni | 1.5 Co | 8 Ru | 1.5 Co | 7 Ni | 3 Co | 50 TaN: and, **e,** 3 Co | 7 Ni | 1.5 Co | 8 Ru | 3 Co | 7 Ni | 1.5 Co | 50 TaN; each with a 20 TaN | 15 Pt underlayer. J=2.5x10^8 A/cm^2 with 5 ns long current pulses. Red and blue symbols correspond to ↑↓ and ↓↑ domain configurations, respectively. The open and solid symbols correspond to positive and negative currents, respectivelyOpen and solid symbols correspond to positive (+x) and negative (-x) current directions, respectively. The error bars shown in

left panels of **a-e** correspond to one standard deviation. All thicknesses are in Å.

To understand the origin of the higher DW velocities in the SAF structures we compare in Fig. 3 the dependence of v on H_x a longitudinal magnetic field applied along the nanowire for various racetracks. We have previously shown that for single layer racetracks (Fig. 3a) the DW velocity goes to zero at a special value of H_x which is largely independent of the driving current, and which takes opposite signs for the ↓↑ and ↑↓ DW configurations. This field reflects an internal magnetic exchange field that the DWs are subjected to and which is considered to be derived from DMI. This interaction results in the DWs exhibiting a chiral Neel structure where the chirality is determined by the interface of the magnetic layer with the underlayer metal. As shown in Fig. 3b the SF racetracks, obtained for thin Ru layers that give rise to F coupling, show an almost identical behavior to the single layer racetracks. Depending on the DW configuration, for a given chirality, the Néel structure is either stabilized by H_x and the DWs go faster, or the Néel structure is destabilized by H_x, and the DWs slow down. This corresponds to whether H_x is parallel or antiparallel to the DMI exchange field.

Remarkably, the SAF racetracks exhibit an entirely distinct behavior with regard to the dependence of DW velocity on H_x that depends on the degree of magnetization compensation as shown in Fig. 3c-e. When poorly compensated the field dependence is similar to that of the single layer and SF structures (Fig. 3c). When the compensation is large enough (Fig. 3d and e) the field dependence of v shows a completely different behavior wherein the DW velocity is decreased for both positive and negative H_x and the behavior no longer significantly depends on the ↓↑ or ↑↓ DW configuration. This behavior can be understood by extending the 1D model of current and field induced DW dynamics to the SAF and SF structures.

2. Dzyaloshiinski-Moriya Interaction (DMI) induced at Co/Ru interface

As discussed above, we find that the DMI fields at Ru/Co and Co/Ru interface are required to be finite (~ -300 Oe for up-down and +300 Oe for down-up configuration) in order to achieve the best fitted results from the velocity ν versus H_x curves (Fig. 2 and 3). To directly measure the DMI field strength H_{DMI}^{Cr} induced at Co/Ru interface, with Kerr microscope we investigated the DW dynamics on the nanowire formed from 15 Å Pt | 3 Å Co | 7 Å Ni | 1.5 Å Co | t_{Ru} Å Ru as a function of H_x for various t_{Ru}.

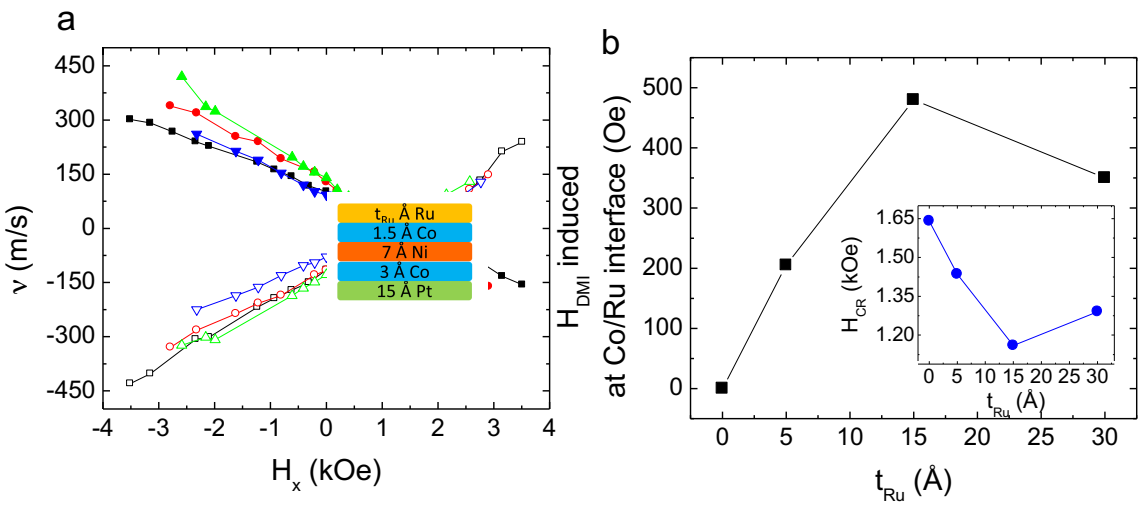

Fig. 4. a. Plot of DW velocity ν versus the longitudinal field Hx for various Ru thickness t_{Ru} measured by Kerr microscope on up-down domain configuration. Black squares (t_{Ru}=0 Å), red circles (t_{Ru}=5 Å), green up-triangles (t_{Ru}=15 Å), and blue down-triangles (t_{Ru}=30 Å). The solid and open symbols correspond to positive and negative current, respectively. b. Plot of H_{DMI} induced from Co/Ru interface obtained from plot **a** as a function of t_{Ru}. The crossing field H_{CR} is plotted in the inset.

The measured DW velocity ν shows a monotonic variation as a function of H_x, as is usually observed in DW motion driven by CST in single domain racetracks (see Fig. 4a). Here the curves show a shift of the crossing field H_{CR}, where the DWs stop moving, with increasing t_{Ru} (also see inset of Fig 4b). The H_{DMI}^{Cr} can be estimated from H_{CR}; $H_{DMI}^{Cr}=H_{CR}(t_{Ru}=0)-H_{CR}(t_{Ru})$, which is plotted in Fig. 4b. H_{DMI}^{Cr} increases for t_{Ru}=0~15 Å, at which the slope η of ν versus H_x curve is observed to increase. The 1D model shows that η is linearly proportional to DW width Δ and weakly proportional to spin Hall torque. Since the Co/Ru interface layer very unlikely produces spin Hall torque, a slight decrease in anisotropy, which increases Δ, should mainly result in the increase of η.

It is known that the DMI strength increases with the increasing anisotropy since DMI and magnetocrystalline anisotropy have the same origin: spin-orbit interaction, and narrower DW favors DMI. Hence, the increase of H_{DMI}^{Cr} as a function of t_{Ru} may be likely due to the proximity induced magnetization at Co/Ru interface. From Fig. 1b, the interpolation shows that H_{DMI}^{Cr} ~ 300 Oe at t_{Ru}=8 Å which quantitatively agrees with our 1D model calculation on SAF structure in the last section.

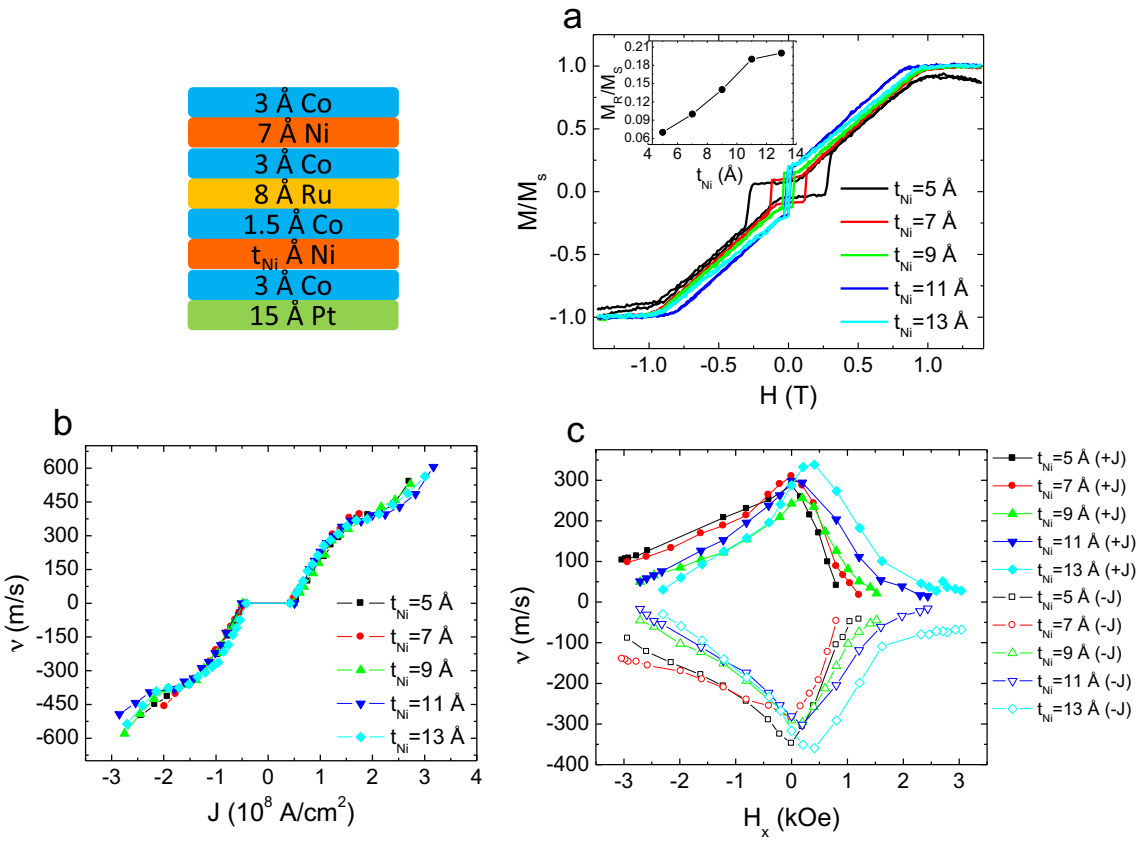

Fig. 5. **a**, Normalized polar Kerr loop measured along the easy axis (out-of-plane) on samples described in the left panel for various t_{Ni}. Plot of DW velocity ν versus **b**, current density J and **c**. the longitudinal field H_x for various t_{Ni} measured by Kerr microscope on up-down domain configuration. **c**, The solid and open symbols correspond to positive and negative current, respectively. **b** and **c**, down-up domain configuration and 2.5 ns pulse length are used, and **c**, J=1.2x10^8 A/cm^2 is used.

3. Tuning spin Hall torque in synthetic antiferromagnet

As discussed in the section 1, in the SAF structure the spin current generated at the Pt/Co interface by SHE attenuates while flowing across the LM and Ru layer to UM, which results in a significant decrease of spin Hall torque on UM and a concomitant reduction of DW velocity. To

study this more systematically, we have measured the DW dynamics in the SAF racetrack nanowires as a function of J and H_x where Ni thickness t_{Ni} in LM only varies as described in Fig. 5b and c. It is expected that the variation of t_{Ni} in Co/Ni/Co does not much change the anisotropy, DMI fields, and exchange coupling field while Co layers interfacing Pt and Ru layers play a key role in CST and ECT driven DW dynamics. As expected, the increase of t_{Ni} decreases M_R/M_S with the increasing t_{Ni} (see Fig. 5a). However, the DW velocity does not change much for various t_{Ni} as a function of J (see Fig. 5b). This can be accounted for by the competition between the decrease of ECT and the increase of spin Hall torque as t_{Ni} increases.

On the other hand, H_x dependence of DW dynamics exhibit systematic changes as a function of t_{Ni} while all showing non-monotonic behavior, a signature of more compensated SAF's Hx dependence as shown in section 1. As t_{Ni} increases, the curves become more symmetric and the peak shifts towards positive H_x, which can be accounted for by the extended 1D model. In particular, when t_{Ni} =5 Å, an abrupt decrease of DW velocity at Hx>0 is observed, which may be due to the formation of Walker breakdown where the M_U keeps on precessing around in x-y plane and M_L oscillates. This Walker breakdown moves DW backwards and forwards in a few tens of pico-seconds time period, thus ending up with heavy slowdown of DW motion. We are presently working on understanding why this interesting phenomenon happens only for SAF racetracks but not in single layer or SF racetracks.

4. Outlook and future plans

We will complete the works discussed in section 2 and 3 above by publication of our results: a paper is under consideration at Nature Nanotechnoogy. The following experiments are planned:

a. Novel Walker-breakdown driven by CST/ECT in SAF structures

b. DMI torque in Ir/Ni and Ni/Ir interfaces

c. Current driven DW motion by vertical thermal gradient in PMA racetracks

d. DW dynamics affected by large vertical electric fields in single layer, SF and SAF PMA racetracks

e. Current driven DW motion in PMA racetracks that contains rare-earth metal layer or ferrimagnets.

References

[1] Ryu, K.-S., Thomas, L., Yang, S.-H. & Parkin, S. Chiral spin torque at magnetic domain walls. *Nat. Nano.* **8**, 527–533 (2013).

[2] K.-S. Ryu, S.-H. Yang, L. Thomas, and S. S. P. Parkin, Nature Commun. Chiral spin torque arising from proximity induced magnetization, **5:3910 doi: 10.1038/ncomms4910** (2014).

[3] Yang, S-H., Ryu, K-S., & Parkin, S. S. P. Giant Exchange Coupling Torque driven Domain Wall velocities in Synthetic Antiferromagnets, under consideration in Nat. Nano.